ISSN 2179-3956

SUPERIMPOSITION OF INDENTATIONS: EXPERIMENTAL APPROACH[1]

Washington Martins da Silva Junior[2]
José Daniel Biasoli de Mello[3]

Abstract

Recent studies state that the wear mechanisms of material removal are connected to the movement of the active particles present at the wear interface. According to tribological conditions, active wear particles slide or roll between surfaces. Particles rolling result in multiple indentations on wear surface. This work presents four experimental methods to evaluate the effect of indentations superimposition in the prevailing wear mechanism. A new device was especially developed to reproduce the abrasive particle interaction. In order to study the effect of superimposition on wear mechanism, series of indentations were created on M2 tool steel sample surfaces by varying the distance between indentations. Analyses were carried out using laser interferometry and SEM. Only one of the methods described in this work presented consistent results that permit the identification of the superimposition degree range, in which wear was observed. Tests showed that a small degree of superimposition results in plastic deformations of the surface. Degrees of superimposition of indentations higher than 50% resulted in mass loss. This method also allows the mapping of the average depth of indentations in function of superimposition degree and normal load of interactions.

Key words: Abrasive wear; Wear mechanisms; Indentation; Superimposition.

SUPERPOSIÇÃO DE INDENTAÇÕES: ESTUDO EXPERIMENTAL

Resumo

Estudos recentes afirmam que o mecanismo de desgaste predominante no desgaste abrasivo está associado com o movimento das partículas atuantes presentes na interface de desgaste. De acordo com as condições tribológicas impostas, as partículas atuantes rolam ou deslizam entre as superfícies. Neste trabalho são apresentados quatro métodos experimentais desenvolvidos para avaliar o efeito da superposição de indentações no mecanismo de desgaste predominante. Um novo equipamento foi projetado especialmente para reproduzir a interação da partícula abrasiva com a amostra. Para estudar os efeitos da superposição no mecanismo de desgaste, séries de indentações foram executadas na superfície de uma amostra de aço ferramenta (tipo M2). O nível de superposição foi controlado ao variar a distância entre as indentações. Análises foram realizadas usando interferometria laser e MEV. Somente um dos métodos descritos neste trabalho apresentou resultados consistentes de perda de material em função da variação do nível de superposição. Resultados mostraram que um baixo nível de superposição de indentações resulta na deformação plástica da superfície. Níveis de superposição maiores que 50% resultaram em perda de massa. Este método também permite o mapeamento da profundidade média das indentações em função do nível de superposição e da força normal dos eventos.

Palavras-chave: Desgaste abrasivo; Mecanismos de desgaste; Indentação; Superposição.

1 *Technical contribution to the First International Brazilian Conference on Tribology – TriboBr-2010, November, 24th-26th, 2010, Rio de Janeiro, RJ, Brazil.*
2 *Centro Tecnológico, Departamento de Engenharia Mecânica, UFES.*
3 *Laboratório de Tribologia e Materiais, Departamento de Engenharia Mecânica, UFU.*

ISSN 2179-3956

1 INTRODUCTION

Studies showed that wear mechanisms are associated with the movement of the particles on the wear interface, and depend on the tribological characteristics of the system.[1-3] Abrasive wear was long ago divided into two main modes: two-body and three-body abrasive wear.[4] More recently, abrasive wear modes have been classified according to the abrasive particle dynamics at the interface:[2] (i) Sliding of active abrasive particles at the interface; (ii) Rolling of abrasives between the surfaces.

During abrasive wear, different wear mechanisms can result in material removal. The sliding of fixed particles or hard protuberances causes scratches on the antagonist surface. A sequence of scratches may be used to simulate the sliding of the particles.[5] Each scratch induces, accordingly to classic literature,[6-8] the mechanisms of microcutting and/or microploughing and/or microcracking.

The rolling of abrasive particles in the interface leads to multiple indentations. The rolling of abrasive particles can be simulated using a sequence of indentations. Each indentation may induce ductile or brittle behavior.[9] Depending of the tribological conditions, particles are able to roll and slide in the interface causing a mixture of indentations and scratches on the surfaces.[5]

Williams and Hyncica[10,11] studied the movement of the particle in lubricated contact. They demonstrated that the main parameters which control the dynamics of the active particle in the interface are: the distances between the surfaces, the size and the shape of the abrasive particles. For a three-dimensional particle, the attack angle increases according to the ratio between the size of the particle and the distance between the surfaces. When the attack angle increases, ploughing is more active, whereas above a critical value the situation changes to one in which there is considerable wear by machining or cutting. Thus, an increase in the attack angle affecting the system severity shows two consequent changes in abrasive wear mechanisms: *indentation (rolling) ➔ microploughing (sliding) ➔ microcutting (sliding).*

Fang et al.[12] highlighted the influence of the shape of the abrasive particle in determining the principal abrasive wear mechanism. These authors studied, experimentally, the behaviour of only one silica particle when it was compressed between two moving metal surfaces. Rounded particles slide only on the antagonist surface while the sharp particles roll between the surfaces. The sliding particle leads to groove/scratch formation on the surface, while the sharp rolling particle produces series of indentations.

In a previous work,[5] the present authors summarized the main tribological variables that control particles dynamics: *particle load*, which is directly related to the normal load applied, the concentration of abrasive in the environment and the size distribution of the particles; *particle geometry*; *hardness ratio between the surfaces*.

A new methodology to represent the movement of abrasive particles using a sequence of well controlled interactions has been developed by Silva and Mello.[9,13] This new method is based on the reproduction of the particle dynamics. An indentation represents the contact of a rolling abrasive particle, which can lead to deformation or cracking, and a scratch represents the sliding of an abrasive particle, which can lead to ploughing, side-fin, wedge formation, cutting or cracking.

Further development[5,14] showed that the simulation of a real surface was only possible using a sequence of variable normal load interactions (indentations or scratches). The normal load controlled the size of the interactions which was related to the size range of the particles that generated the reference surface. These

ISSN 2179-3956

results[14] showed that the superimposition of indentations has a great effect on the morphology and topography of the simulated surfaces. In fact, the abrasive wear simulation was only possible using the concept of average depth of superposed interactions.
This work details four experimental methods to evaluate the effect of indentations superimposition on the average depth of indentations. Only one of the methods described in this work showed consistent results that permit the identification of the superimposition degree range in which wear was observed. This method also allowed the mapping of the average depth of indentations regarding the superimposition degree and the normal load of interactions. This mapping was further used in the simulation of abrasive wear in which the rolling of particles prevails.

2 MATERIALS AND METHODS

Figure 1 shows the micro-simulator, a device which was especially developed to reproduce the abrasive particle interaction. Two high resolution (0.1 µm) sliders drive the sample horizontally while a Vickers indenter is moved vertically by another slider (slider z), also with a resolution of 0.1 µm. Besides this, a piezoelectric translator (PZT) was used to control the indenter movement with a resolution of 5 nm for a maximum travel distance of 40 µm. A 3D load cell controls the intensity of the normal load and measures the applied loads and moments in the directions x, y and z. The resolution of the load cell is 0.001 N and the maximum load is 18 N. A specific developed Labview® interface controls the movements of the sample and indenter.

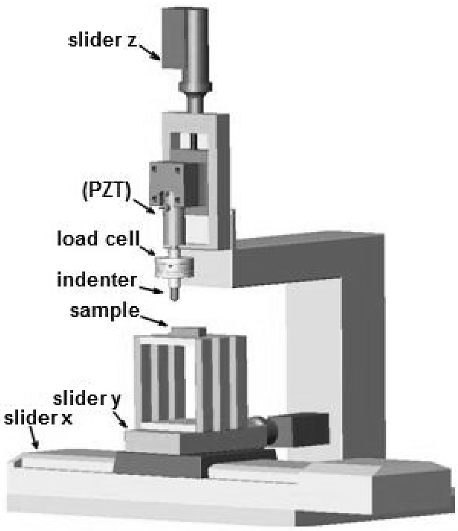

Figure 1- Schematic representation of the micro-simulator.

In this work, M2 tool steel samples (HV = 6.8 GPa) were used. The samples were mirror-polished before the tests. Initially, tests with individual indentations at different normal loads were performed to establish the correlation between normal load and indentation width. Indentation width was measured using optical microscopy. In order to study the superimposition effect of indentations, sequences of indentations, with the same distance between each other, were executed. The aim is to measure the average depth of superposed indentations. The groups of indentations were organized in four different patterns.

ISSN 2179-3956

2.1 Lines of Indentations

A sequence of parallel lines of indentations was produced. The separation between the indentations was reduced between subsequent lines until all the indentations were in the same position. The scheme of the indentations positioning is presented in Figure 2. All the indentations were produced using the same normal load which means a specific square area for each indentation mark (IW – indentation width). The percentage of superimposition is calculated from the ratio between the distance between indentations (DI) and the width of the indentation mark (IW). A degree of superimposition of zero means that the indentations are touching each other. Negative values mean that the indentations are distant from each other by a percentage of one indentation side. The test conditions used in this simulation method will be further presented in section 3.2 (Figure 7).

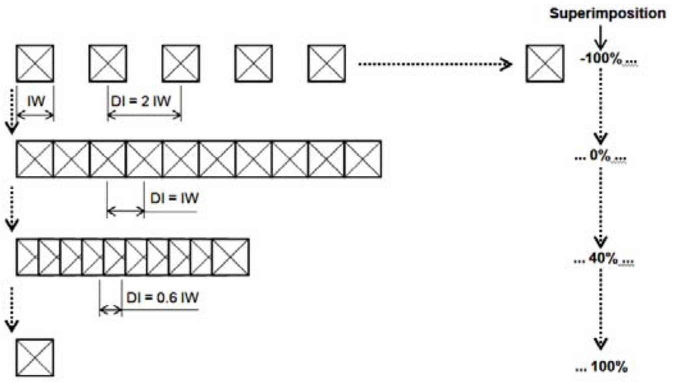

Figure 2- Scheme of indentation positioning in lines.

2.2 Lines of Indentations Varying the Number of Indentations

Analogous to the previous method, a sequence of parallel lines of indentations was produced, but now the length of the line of indentations has a fixed value. In order to vary the degree of superimposition, the amount of indentations was increased progressively, decreasing the distance between indentations, as shown in Figure 3. Table 1 summarizes the conditions used in the simulations using lines of indentations increasing the density of indentations.

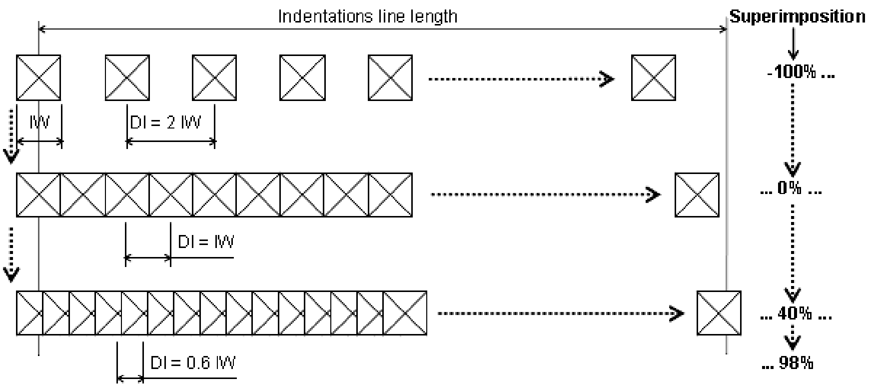

Figure 3- Schematic representation of indentation lines with different number of indentations.

Table 1. Test conditions for the superimposition tests using lines of indentations.

S %	-100	-50	-30	-10	0	10	20	30	40	50	60	70	80	90	98
NI	8	11	13	15	16	18	20	23	27	33	41	54	82	163	817
DI (µm)	36.7	27.5	23.8	20.2	18.3	16.5	14.7	12.8	11.0	9.2	7.3	5.5	3.8	1.8	0.4

S = Degree of superimposition; NI = number of indentations; DI = distance between indentations.

ISSN 2179-3956

2.3 Areas of Indentations

For this method, a sequence of squared areas of indentations was produced keeping the same number of indentations in each area. In order to increase the degree of superimposition, the separation between the indentations was reduced, between subsequent areas, until all the indentations were in the same position. The scheme of the indentations positioning is presented in Figure 4. The test parameters for the simulation with controlled superimposition are presented in Table 2.

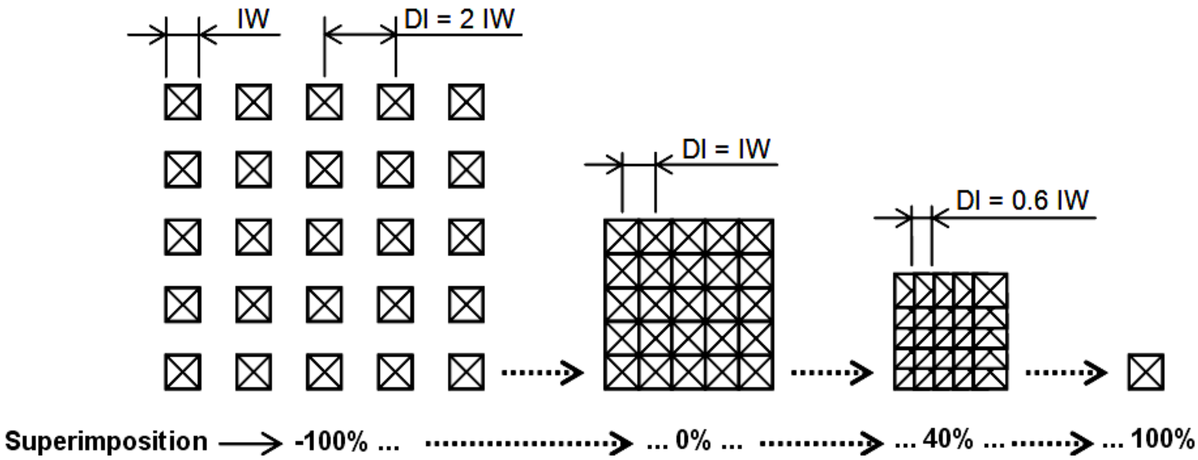

Figure 4- Scheme of indentation positioning.

Table 2. Testing conditions for areas of indentations

S %	-100	-50	0	10	20	30	40	50	60	70	80	90	100
NI	100	100	100	100	100	100	100	100	100	100	100	100	100
DI (µm)	36.7	27.5	18.4	16.5	14.7	12.8	11.0	9.2	7.3	5.5	3.7	1.8	0.0

S = Degree of superimposition; NI = number of indentations; DI = distance between indentations.

2.4 Areas of Indentations Varying the Number of Indentations

In this method, a sequence of same size squared areas of indentations was produced. The degree of superimposition was controlled increasing the density of indentations between the subsequent areas. The scheme of the indentations been positioned is presented in Figure 5. In this case, the maximum degree of superimposition was of 85% because the number of indentations increased exponentially, limiting the execution of the test, as shown in Table 3.

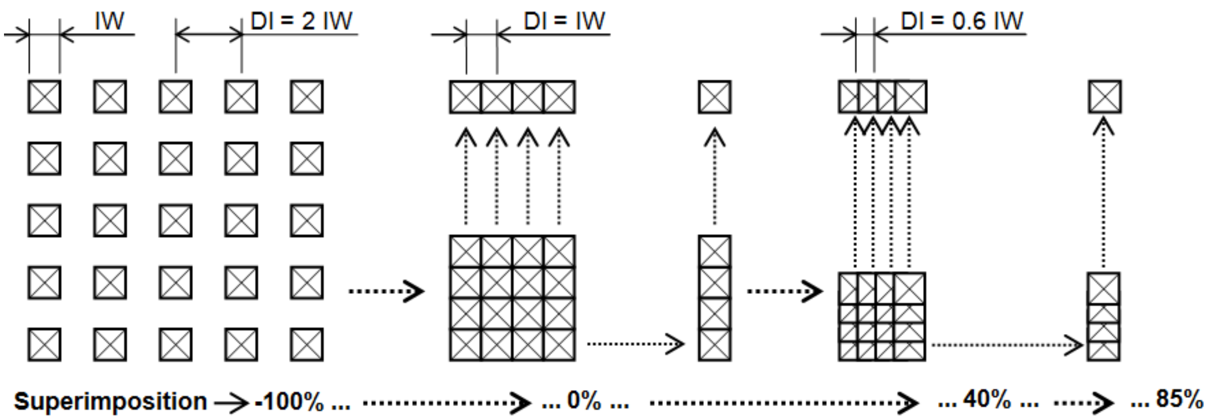

Figure 5- Area positioning scheme for superimposition tests increasing the density of indentation.

ISSN 2179-3956

Table 3. Superimposition tests conditions for same sized area of indentations

S %	-100	-50	-20	0	20	40	50	60	70	80	85
NI	25	49	81	121	196	324	484	729	1296	2916	5329
DI (µm)	36.7	27.5	22.0	18.4	14.7	11.0	9.2	7.3	5.5	3.7	2.7

S = Degree of superimposition; NI = number of indentations; DI = distance between indentations.

3 RESULTS AND DISCUSSION

3.1 Normal Load and Individual Indentation width Relationship

In order to establish the correlation between normal load and indentation width, tests with individual indentations at different normal loads were performed, as shown in Figure 6. The width measurements were performed using optical microscopy.

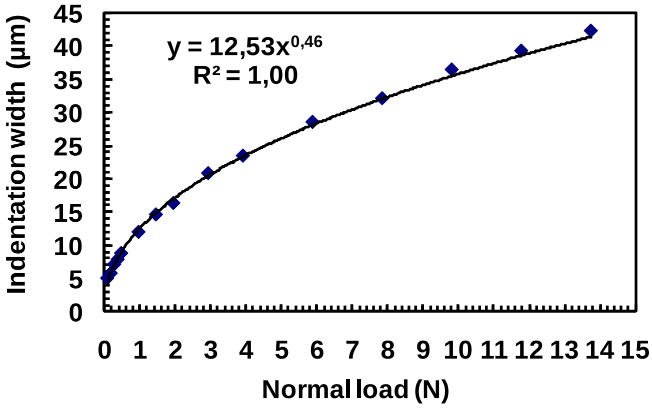

Figure 6- Indentation width as function of normal load for monoindentations.

This relationship allows the control of the indentation area, defined by the normal load imposed during the interaction. In superimposition tests, the degree of superimposition was defined by the ratio of the single indentation width value and the distance between indentations.

3.2 Superimposition Tests

Figure 7 shows the superimposition test result obtained using the methodology proposed in the section 2.1. In this exploratory test, 19 different superimposition conditions and ten indentations in a roll were used.
The normal load of these indentations was fixed in 1.5 N which corresponds to an indentation width of 14.9 µm width according to the relation showed in figure 6. The topographical profile, measured using laser interferometry (LI), of the lines “AA” and “BB” illustrated in Figure 7, are presented in Figure 8.
Profile “AA” (Figure 8a), shows that, for this condition, indentations are not superposed and the depths of indentations are quite similar. However, for the test condition represented by the profile “BB” (Figure 8b), the depth of the last indentation is pronounced in comparison to the group of indentations. In the last case (Figure 8b), the average depth of indentations is low in comparison to the non-superposed indentation depth (Figure 8a). This result can be explained by the fact that one indentation can partially fulfill the mark left by the previous indentation. This fact led to the decrease of the average depth of indentations. Figure 9 shows the average depth of indentations obtained in all indentation lines.

ISSN 2179-3956

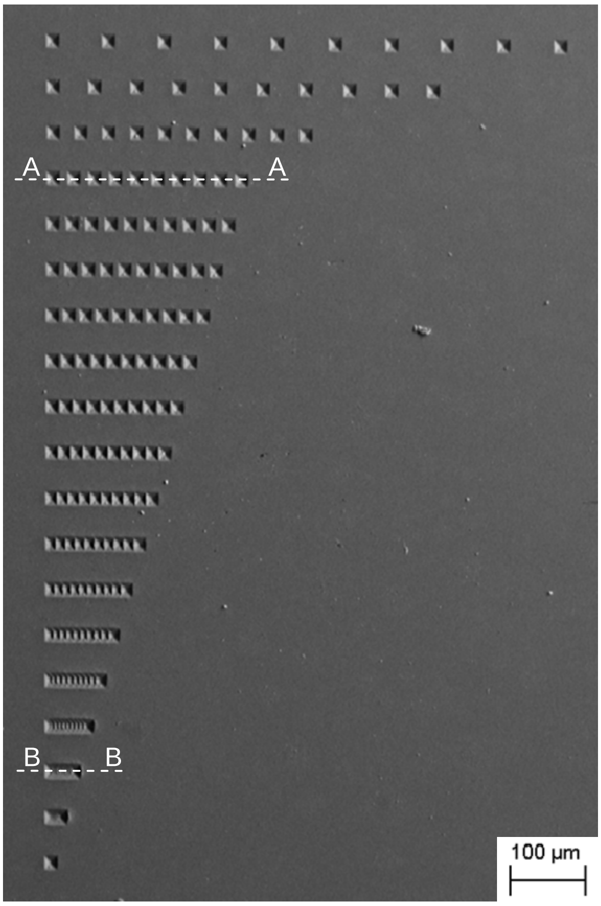

Distance between indentations	Superimposition
59.6 µm	-300%
44.7 µm	-200%
24.8 µm	-100%
22.3 µm	-50%
20.9 µm	-40%
19.4 µm	-30%
17.9 µm	-20%
16.4 µm	-10%
14.9 µm	0%
13.4 µm	10%
11.9 µm	20%
10.4 µm	30%
8.9 µm	40%
7.4 µm	50%
5.9 µm	60%
4.5 µm	70%
2.9 µm	80%
1.5 µm	90%
0 µm	100%

Figure 7- Superimposition tests using lines of indentation keeping the same number of indentations in each line. SEM.

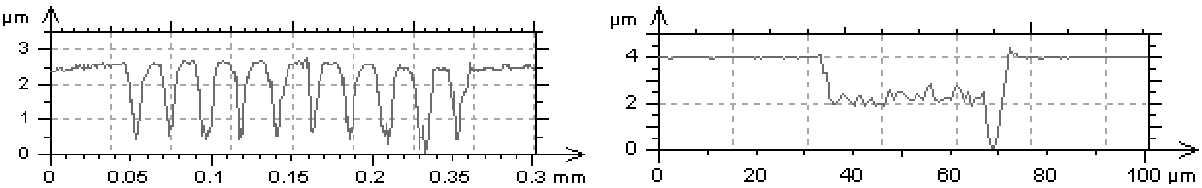

-a- -b-

Figure 8- Topographical profile: a- “AA”, degree of superimposition -50% and b- “BB”, degree of superimposition 80%. LI.

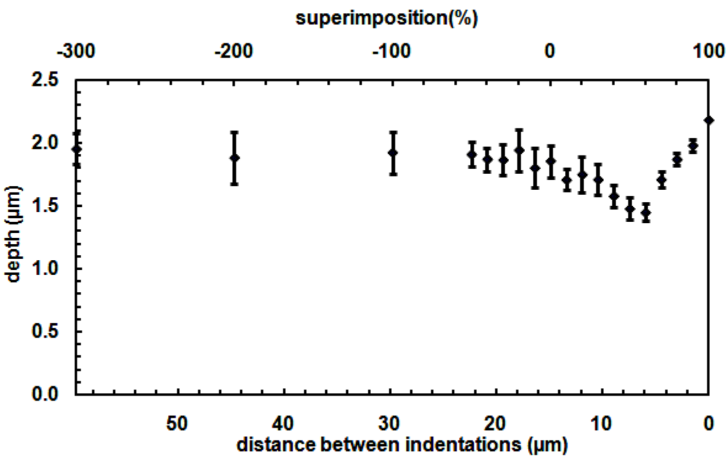

Figure 9- Effect of the superimposition in the average depth of indentations.

ISSN 2179-3956

For degree of superimposition higher than 0%, the indentations are superposed, the average depth decreases until 60% of superimposition due to the deformation process. After that, the average depth increases until the last line, when all indentations are in the same position. The profile “BB” (Figure 8b), shows that for a higher degree of superimposition, the dimension of the last indentation is considerably big comparing to the size of the line of indentations. In addition, Figure 7 shows that while the degree of superimposition increases, the length of the indentations lines decreases. These two facts induced errors in the average depth measurement for a high degree of superimposition.
The results of the method detailed in section 2.2 are shown in Figure 10. In this test, the maximum length of the line of indentation was fixed in 300 µm and the number of indentations increased in subsequent lines composing 15 different degrees of superimpositions.

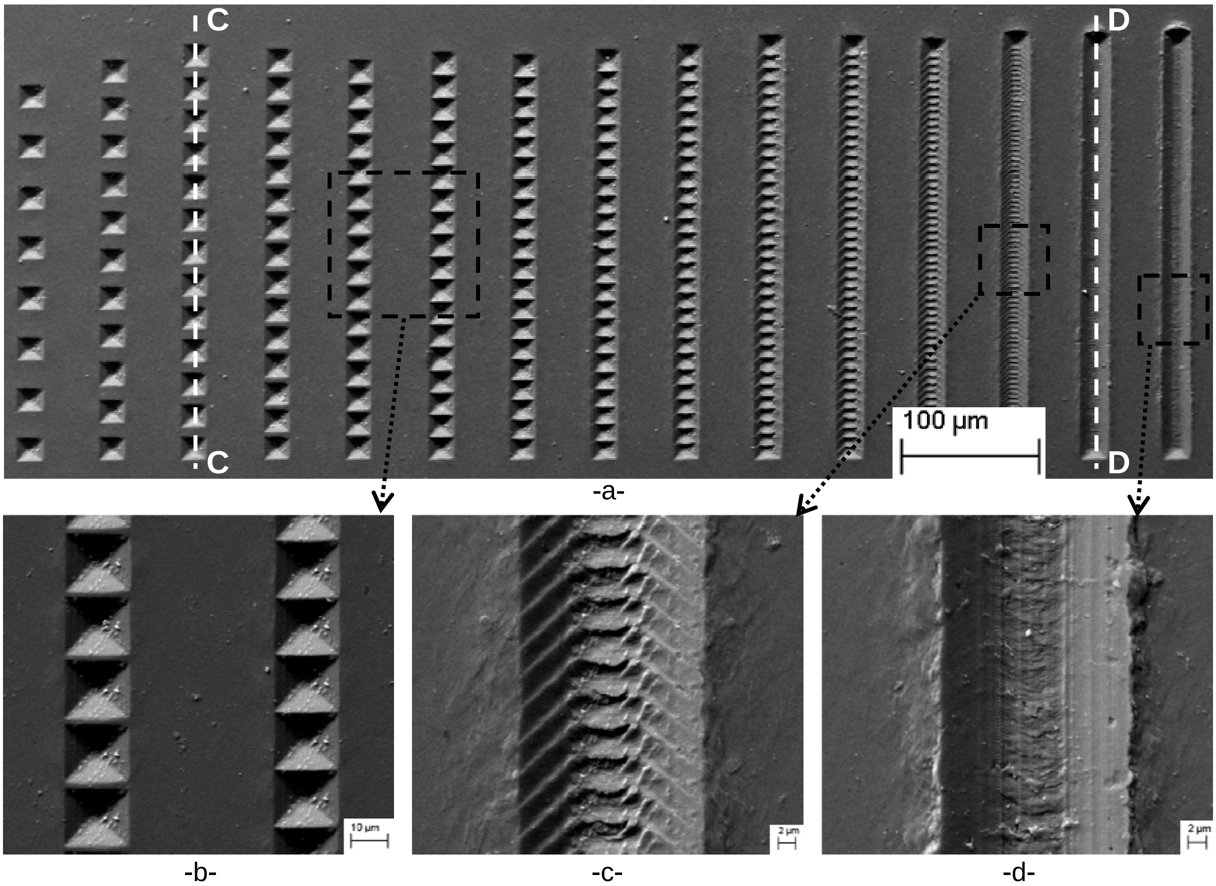

Figure 10- a- Lines of indentations increasing the density of indentation. Superimposition degree: b- 0% and 10%; c- 80%; d- 98%. SEM.

The normal load of the indentations was fixed in 2.3 N which corresponds to a width of 18.35 µm according to the relation showed in figure 6. In this test, the maximum degree of superimposition was limited in 98% because the number of indentations in a roll increases fast due to the superimposition degree (Table 1).
Figure 11 shows the topographical profiles marked in Figure 10 obtained using laser interferometry. Comparing profile DD and profile BB (Figure 8b), in this method the size of the last indentation does not affect the measurement of the average depth of superposed indentations.

ISSN 2179-3956

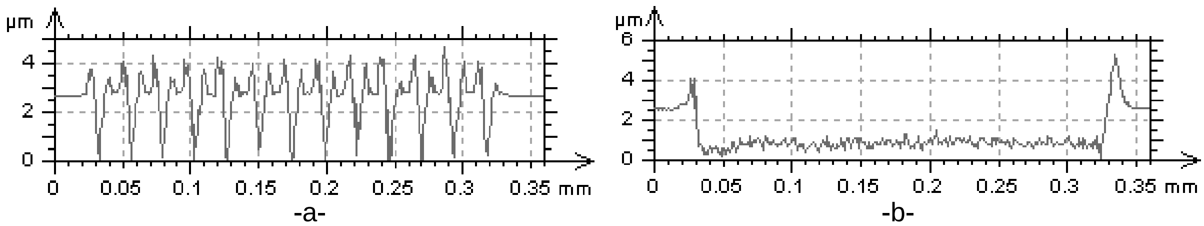

Figure 11- Profiles in different superimposition degree: a- -30% ("CC"); b- 90% ("DD"). LI.

Using a specific software (Mountains Map Universal® – Digital Surf) to analyze those profiles, the average depth of indentations and the deformed area above and below the surface were measured and presented in Figure 12.

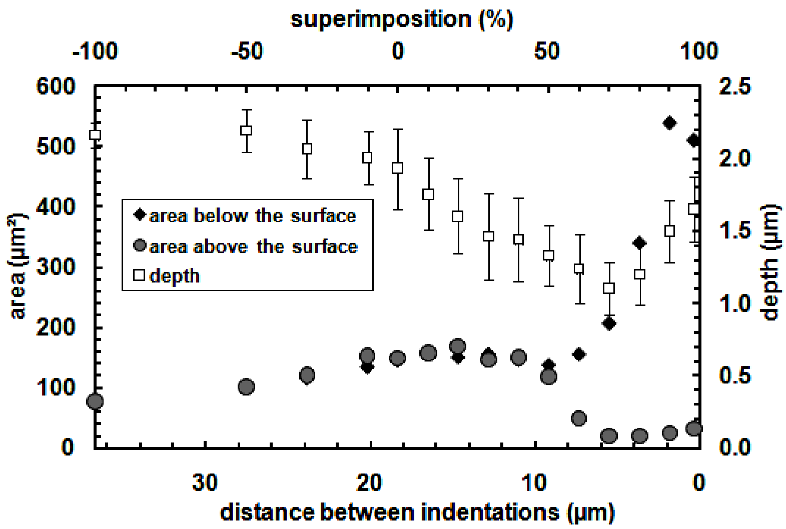

Figure 12- Average depth of superposed indentations and variation of the areas above and below the sample surface in function of the degrees of superimposed lines of indentations.

The depth of superposed indentations, measured using the surface of the sample as reference, behaved just like the method had previously presented, figure 9. This suggests that the material deformed by an indentation partially fulfills the mark left by previous indentations.

The values of deformed material above and below the surface of the sample are very similar until a degree of superimposition of around 50%, Figure 12. In this region, the material deformed by the indentations was probably displaced to the sides of the events. For superimpositions larger than 50%, the area above the reference line increased sharply, suggesting material removal caused by intense repeated deformation. These results strongly indicate that it is possible to simulate material removal in ductile materials using superimposed indentation tests when the particle dynamics in the system to be simulated involves rolling and therefore repeated indentation of the surface.

Figure 13 shows the superimposition test result obtained using the methodology detailed in the section 2.3. In this test, one hundred indentations were executed in a squared area, changing the distance between indentations in subsequent areas. The normal load was fixed in 2.3 N which corresponds to an indentation width of 18.35 μm. The positions of the first and last lines and of the last indentation are indicated in the Figure 13.

In each area, the average depth of indentations was measure using at least seven topographical profiles. These results are shown in the Figure 14.

ISSN 2179-3956

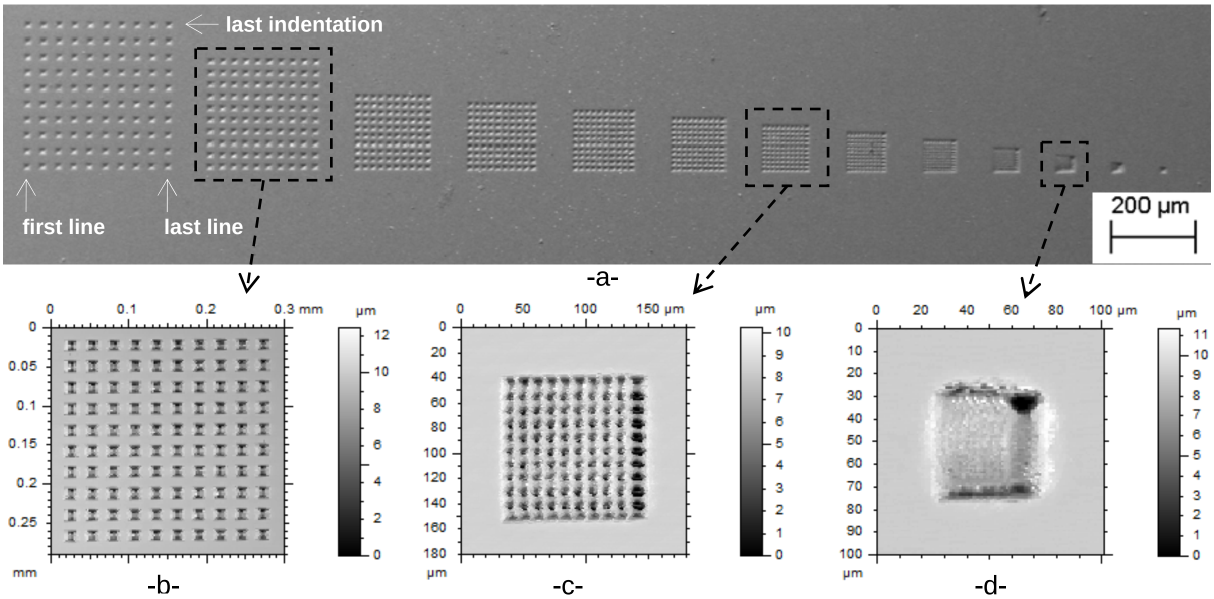

Figure 13- a- Superimposition tests using areas: b- -50%; c- 40%; d- 80%, SEM / LI.

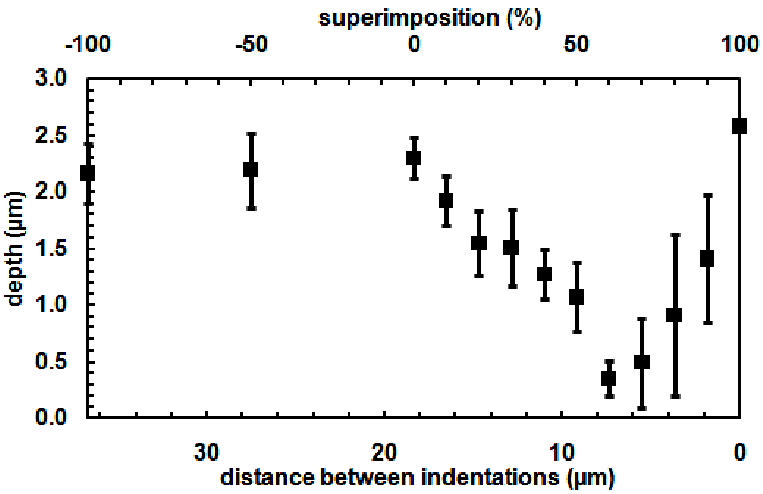

Figure 14- Average depth of indentations measured in areas with different superimposition degree.

The effect of the size of the last line of indentation was pronounced for areas with a degree of superimposition higher than 40%, as shown in Figures 13c and d.
In this case, the deformation process contributed to fulfill the previous indentation marks in two ways: *inside the line*, when one indentation partially covers the previous; *between lines*, when one line of indentation partially covers the previous.
In consequence, a strong decrease of the average depth was observed after 0% of superimposition, until around 60% of superimposition, as shown in Figure 14.
Analogous to the method detailed in section 2.1, the effect of the size of the last line and the fast decrease of the size of the area, induced errors on the average depth measurements.
The results of the method detailed in the section 2.4 are shown in the Figure 15. The normal load was fixed in 2.3 N (mark width of 18.35 µm). The area of indentations was fixed in 200 x 200 µm and the number of indentations was increased in subsequent areas in 11 different degree of superimposition. The maximum degree of superimposition was limited in 85% because the number of indentation per area increases strongly in function of superimposition degree (Table 3).

ISSN 2179-3956

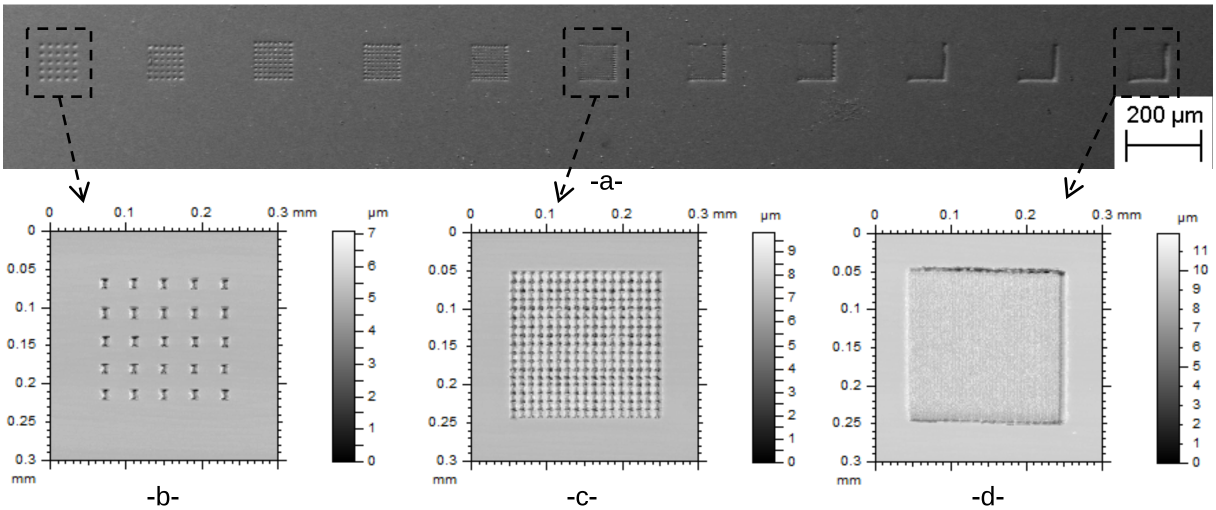

Figure 15- a- Areas of indentations in different superimposition degrees. b- -100%; c- 40%; d- 85%. SEM / LI.

In this method the measurement problem caused by the size of the last indentation was minimized and it is perfectly possible to measure the average depth of superimposed surface. For that, some profiles (at least seven), were taken from each area and the average depth of the profile was measured. These results are shown in the Figure 16.

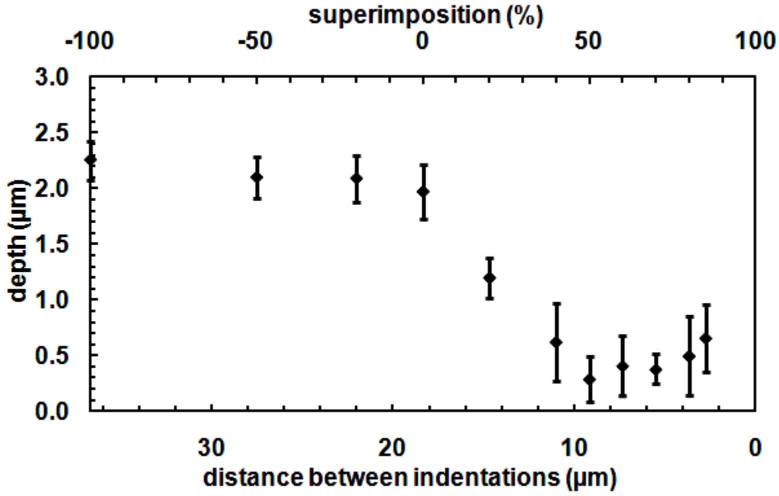

Figure 16- Average depth of indentations obtained in areas with increased density o indentations.

Again, the superimposition of indentations affects the average depth of indentations after 0% of superimposition, decreasing the depth values until 50% of superimposition. After that, results showed a slight increase in the average depth.
In this test, measurements of the deformed area above and below have not showed a consistent correlation.

4 CONCLUSIONS

The aim of this work was to show the development of a method to measure the average depth of superimposed indentations. This physical parameter will be further used to control a simulation of abrasion involving rolling of particles and therefore repeated indentation of the surface.
All methods presented in this work showed that the average depth of indentations was affected after 0% of superimposition, because in this condition the area of

indentation marks superimposed one another, leading to an intense deformation process.
The method "lines of indentations increasing the density of indentations" showed a good correlation between the average depth of indentations and the degree of superimposition. Additionally, measurements of the deformed areas above and below the surface allowed the identification of wear, which occurs in degrees of superimposition higher than 50%. This method can be applied on different materials to indentify the critical value of superimposition which induces wear.

Acknowledgements

The authors are grateful to Capes/Brazil for the scholarship offered to W. M. da Silva and to CNPq/Brazil for the financial support.

REFERENCES

1 ADACHI, K.; HUTCHINGS, I. M. Wear mode mapping for the micro-scale abrasion test, **Wear**, v. 255, p. 23-29, 2003.
2 TREZONA, R. I.; ALLSOPP, D. N.; HUTCHINGS, I. M. Transition between two-body and three-body abrasive wear: influence of test conditions in the microscale abrasive wear test, **Wear**, v. 225-229, p. 205-214, 1999.
3 DA SILVA, W. M.; BINDER, R.; DE MELLO, J. D. B. Abrasive wear of steam treated sintered iron, **Wear**, v. 258, p. 166-177, 2005.
4 BURWELL, J. T. Survey of Possible Wear Mechanisms, **Wear**, v. 1, 119 – 141, 1957.
5 DA SILVA, W. M.; DE MELLO, J. D. B. Using parallel scratches to simulate abrasive wear, **Wear**, v. 267, p. 1987–1997, 2009.
6 GODDARD, J.; WILMAN, H. A theory of friction and wear during the abrasion of metals, **Wear**, v. 5, Issue 2, p. 114-135, 1962.
7 SEDRIKS, A. J.; MULHEARN, T. O. Mechanics of cutting and rubbing in simulated abrasive process, **Wear**, v. 6, pp 457 – 466, 1963.
8 ZUM GAHR, K. L. **Microstructure and wear of materials**, Tribology Series, v. 10, ELSEVIER SCIENCE PUBLISHERS B. V., Amsterdam, ISBN 0444427546, 560 p, 1987.
9 SILVA, W. M.; MELLO, J. D. B. Ductile-to-Brittle Transition During Abrasive Wear Evaluated Using Multiple Interaction Simulations, **Proceedings of CIST2008 & ITS-IFToMM2008**, September 24th to 27th, Beijing, China, 2008.
10 WILLIAMS, J. A.; HYNCICA, A. M. Mechanisms of abrasive wear in lubricated contacts, **Wear**, v. 152, p. 57-74, 1992.
11 WILLIAMS, J. A.; HYNCICA, A. M. Abrasive wear in lubricated contacts, **J. Phys. D: Appl. Phys.**, v. 25, p. A81-A90, 1992.
12 FANG, L.; KONG, X. L.; SU, J. Y.; ZHOU, Q. D. Movement patterns of abrasive particle in three-body abrasion, **Wear**, v. 162 - 164, p. 782 – 789, 1993.
13 SILVA, W. M.; MELLO, J. D. B. Simulação de Desgaste Abrasivo via Eventos Múltiplos, **Ciência & Tecnologia dos Materiais** (ISSN: 0870-8312), 18, Issue 1/2, p. 49-56, 2006 – in Portuguese.
14 SILVA, W. M.; MELLO, J. D. B. Método de Simulação do Desgaste Abrasivo Usando Interações Múltiplas, 64TH ANNUAL CONGRESS OF ABM - BRAZILIAN METALLURGY ASSOCIATION, **Proceedings of 64th annual ABM Congress**, July 13th to 17th, Belo Horizonte, MG, Brazil, 2009 – in Portuguese.